

Evaluation of a new imaging software for aortic endograft planning

G. TINELLI¹, A. HERTAULT², T. MARTIN GONZALEZ², R. SPEAR², R. AZZAOU^{1,2}, J. SOBOCINSKI², R.E. CLOUGH², S. HAULON²

¹UOC di Chirurgia Vascolare, Polo CardioVascolare e Toracico, A. Gemelli Foundation, Catholic University of the Sacred Heart, Rome, Italy

²Aortic Centre, Hôpital Cardiologique, Lille University Hospital, Lille, France

Abstract. – OBJECTIVE: The aim of this study was to evaluate a new 3D Workstation workflow (EVAR Assist, Advantage Windows, GE Healthcare, Chalfont, UK) (EA-AW) designed to simplify complex EVAR planning.

PATIENTS AND METHODS: All pre-operative computed tomography (CT) scans of patients who underwent repair at our institution of a complex aortic aneurysm using fenestrated endovascular repair (f-EVAR) between January and September 2014, were reviewed. For each patient, imaging analysis (12 measures: aortic diameters and length and “clock position” of visceral artery) was performed on two different workstations: Aquarius (TeraRecon, San Mateo, CA, USA) and EA-AW. According to a standardized protocol, three endovascular surgeons experienced in aortic endograft planning, performed image analyses and data collection independently. We analyzed an internal assessment between observers (on the Aquarius 3DWS) and an external assessment comparing these results with the planning center (PC) data used to custom the fenestrated endograft of the patients enrolled in this study. Finally, we compared both 3DWS data to determine the accuracy and the reproducibility. A p -value $< .05$ was considered as statistically significant. Complete agreement between operators was defined as 1.0.

RESULTS: Intra- and inter- observer variability (interclass correlation coefficients – ICC: 0.81-.091) was very low and confirmed the reliability of our planners. The ICC comparison between EA-AW and Aquarius was excellent (> 0.8 for both), thus confirming the reproducibility and reliability of the new EA-AW application. Aortic and iliac necks diameters and lengths were similarly reported with both workstations. In our study, the mean difference in distance and orientation evaluation of target vessels evaluated by the two workstations was marginal and has no impact on clinical practice in term of device manufacturing.

CONCLUSIONS: We showed that complex EVAR planning can be performed with this new

dedicated 3D workstation workflow with a good reproducibility.

Key Words:

Endovascular planning, 3D work station, Complex aortic aneurysms, FEVAR, Fenestrated graft.

Introduction

Careful preoperative planning is a key to ensure technical success and favorable long-term outcomes after endovascular aortic aneurysm repair (EVAR). Evidence in the literature suggests that routine use of 3D workstations for EVAR planning significantly reduces the rate of type 1 endoleaks and the rate of secondary interventions^{1,2}. Juxta-, para-renal and thoraco-abdominal endovascular aortic aneurysm repair require a proximal sealing zone above the visceral arteries, in a non-diseased segment of the aorta. Perfusion of the visceral arteries is maintained by fenestrations or branches of the aortic endograft. Accurate preoperative analysis is thus mandatory to: (1) locate the proximal landing zone to achieve good fixation and sealing; (2) determine the exact position of the visceral arteries, also called “target vessels” (renal arteries, superior mesenteric artery [SMA], celiac trunk [CT]), that will be perfused through fenestrations and/or branches³. Designing such complex devices requires a substantial level of experience and expertise in the analysis of pre-operative images. 3D-workstations (3DWS), allowing multiplanar, curvilinear and 3D reconstructions of pre-operative images, are now routinely used by endovascular therapists to conceive custom-made endografts, matching perfectly patients’ anatomy, or to plan step-by-step endovascular procedures. Many

3DWS are commercially available; the Aquarius workstation (TeraRecon, San Mateo, CA, USA) is our reference standard to design such complex endografts⁴⁻⁶. These 3D workstations need to be intuitive, “user-friendly”, and integrate dedicated workflows for standard and complex EVAR. With the uprising of modern hybrid rooms, fusion imaging is used routinely by endovascular therapists. It has been associated with significant reduction of X-ray exposure and contrast-medium injection during endovascular procedures^{7,8}, and provides a continuous guidance that facilitates complex procedures. However, no workstation offers a continuous workflow incorporating endograft sizing and procedure planning, including fusion mask preparation. Currently, a new 3D imaging analysis is required the day of the procedure, resulting in additional work, and a loss of time and information that was already available during the planning process. To overcome this clinical need, a new workflow integrating endograft conception, procedure planning and fusion preparation on a unique 3D workstation (Flight plan for EVAR, Advantage Windows, GE Healthcare) was developed. The aim of this study was to evaluate that the planning process for complex EVAR integrated into this new 3DWS workflow was similar compared with the standard planning in term of measurements reproducibility.

Patients and Methods

Study Group

Pre-operative computed tomography (CT) scans of all patients who underwent endovascular repair for juxta-, para-renal or thoraco-abdominal aortic aneurysms using fenestrated endografts (f-EVAR) at a single institution between January and September 2014, were retrospectively analyzed. Patients with aortic dissection, patients treated with devices including branches or patients with a preoperative CT scan with slice thickness greater than 1.00 mm or poor injection quality were excluded. All endografts were provided by the same manufacturer (Cook Medical, Bloomington, IN, USA). The Ethical Committee approved this retrospective study. Written informed consent for the procedure was obtained from all patients.

Imaging Analysis

For each patient, imaging analysis was performed on two different workstations: Aquarius (TeraRecon, San Mateo, CrA, USA) and EVAR Assist

(Advantage Windows, GE Healthcare, Chalfont, UK) (EA-AW). The first step consisted of automatic reconstructions of the aorta in multiplanar (MPR), maximum intensity projection (MIP) and 3D volume rendering (VR) reconstructions. Centerlines of flow (CLF) were then automatically generated for the aorta and its main branches. CLF were always checked and manually edited if required. The third step was the creation of a “stretched view” from the CLF to perform accurate lengths and diameters measurements. This “stretched view” image is rotated on its centerline axis to accurately identify the center of each target vessel ostium. Target vessels “clock positions” were measured on cross-section views, perpendicular to the CLF. The superior mesenteric artery ostium clock position was defined as the 0° position. Image analyses and data collection were performed independently by three endovascular surgeons experienced in aortic endograft planning (G.T., A.H., and T.M.G.), according to a standardized protocol. Variables listed in Table I were measured. Distances involving target vessels were measured from the center of the ostium of each vessel, with the exception of hypogastric arteries where the top of the vessel origin was considered (Figure 1). All measurements were compared to those provided by the planning center (PC) that designed the fenestrated endografts of the patients enrolled in this study. This study was conducted according to the STARD (Standards for Reporting of Diagnostic Accuracy) initiative for diagnostic accuracy⁹.

Statistical Analysis

Continuous variables were expressed as mean with standard deviation (SD) or median with range, according to data distribution (parametric or nonparametric, respectively). For continuous variables, inter-observer reliability was assessed between each operator on the Aquarius workstation using interclass correlation coefficients (ICCs), and variation between data sets was compared by calculating the mean pair difference for each data point and averaging them for the dataset comparison. Comparisons between observers were made with ANOVA test for continuous variables. Mean score between the three observers was compared with post-hoc comparisons using the Tukey HSD test. External assessment was performed by direct comparison between the means of the three operator’s measurements and data provided by the planning center on the Aquarius workstation. The EA-AW workstation accuracy was evaluated by correlation assessment between

Table I. List of the different measurements performed on the 3D workstations.

Variables of interest	Definition
R1	Distance from the SMA to the right renal artery*
R2	Distance from the SMA to the left renal artery*
iRR	Distance between renal arteries
L1	Distance from the lowest renal artery to the aortic bifurcation
L2	Distance from the aortic bifurcation to the right hypogastric artery
L3	Distance from the aortic bifurcation to the left hypogastric artery
D1	Maximum aortic diameter 20mm above the SMA ostium
D2	Right common iliac artery diameter (10mm above the iliac bifurcation)
D3	Left common iliac artery diameter (10mm above the iliac bifurcation)
cp-CT	Celiac trunk clock position
cp-RR	Right renal clock position*
cp-LR	Left renal clock position*

In the setting of two ipsilateral renal arteries, the lowest was considered.

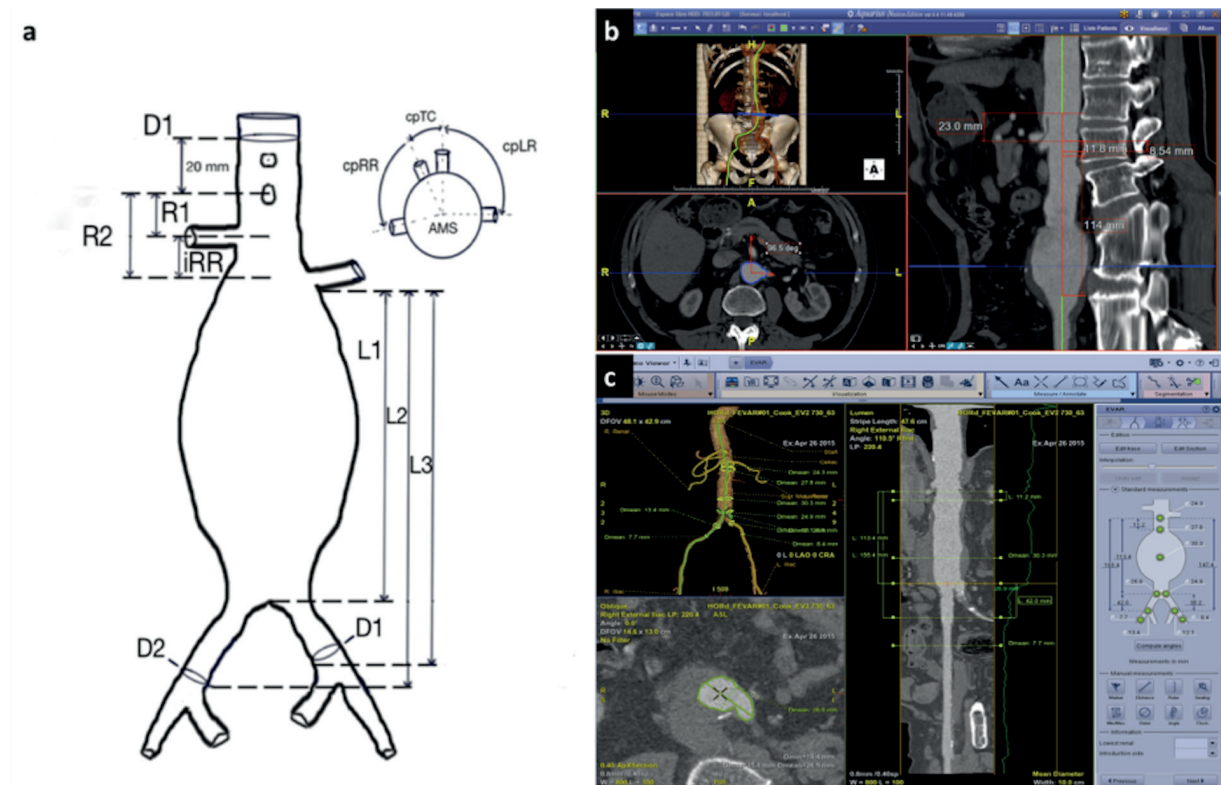


Figure 1. Para-renal abdominal aortic aneurysm morphometry: (a) diameters and length measurements (b) screen captures of a semi-automatic sizing performed on an Aquarius 3DWS (TeraRecon, San Mateo, CA, USA) (c) and on EVAR Assist (Advantage Windows, GE Healthcare, Chalfont, UK).

measurements on both workstations for each operator. A p -value < 0.05 was considered as statistically significant. Complete agreement between operators was defined as 1.0. Statistical analysis was performed using SPSS version 22.0 (IBM Armonk, NY, USA).

Results

Among the 51 consecutive patients treated by f-EVAR during the study period, 29 patients matched the inclusion criteria. Excluded patients were:

- 4 dissections aortic disease;

Table II. Reproducibility between operators – Measurements were performed on 29 preoperative CT-scan by three independent operators on the Aquarius workstation (Terarecon) (* $p < 0.0005$ for all comparisons). ICC: Interclass Correlation Coefficients, CT: Celiac Trunk, SMA: Superior Mesenteric Artery, RR: Right Renal, LR: Left Renal.

Measure		ICC (CI 95%)* Operators		
		1 vs. 2	1 vs. 3	2 vs. 3
Clock Positions (Absolute value)	CT	.80 (.58 - .91)	.84 (.66 - .92)	.83 (.63 - .92)
	SMA	.81 (.59-.91)	.81 (.60-.91)	.87 (.73-.94)
	RR	.81 (.59-.91)	.86 (.71-.93)	.70 (.36-.86)
	LR	.82 (.62-.92)	.90 (.78-.95)	.73 (.42-.87)
Clock positions (SMA at 0°)	cp-CT	.89 (.78-.95)	.82 (.62-.91)	.79 (.55-.90)
	cp-RR	.81 (.59-.91)	.70 (.37-.86)	.62 (.20-.82)
	cp-LR	.81 (.59-.91)	.81 (.60-.91)	.75 (.47-.88)
	R1	.94 (.88-.97)	.98 (.96-.99)	.93 (.86-.97)
Distances between SMA renal arteries	R2	.99 (.97-.99)	.99 (.97-.99)	.98 (.96-.99)
	iRR	.94 (.86-.97)	.95 (.96-.99)	.94 (.86-.97)
	D1	.74 (.46-.88)	.91 (.81-.96)	.76 (.50-.89)
Aortic and iliac diameters (sealing zones)	D2	.97 (.94-.99)	.95 (.90-.98)	.93 (.84-.96)
	D3	.89 (.78-.95)	.92 (.84-.96)	.76 (.50-.88)
	L1	.96 (.92-.98)	.99 (.98-.99)	.95 (.90-.98)
Distance from the lowest renal to the aortoiliac bifurcation	L2	.97 (.95-.99)	.99 (.98-.99)	.97 (.95-.99)
	L3	.98 (.95-.99)	.98 (.97-.99)	.96 (.91-.98)
Common iliac lengths				

– 16 patients with insufficient CT scan quality for the present study (slice cut > 1 mm or poor quality of injection).

The patients enrolled were 25 man and 4 women, respectively. The average age was 71.09 years (range 65-78 years). All cases were treated for aneurysmal disease of abdominal aorta (> 6 cm).

1) Reproducibility between operators: comparison operator to operator on the Aquarius workstation (Internal assessment)

Internal assessment on the Aquarius workstation showed no statistical difference between the three operators regarding aortic and iliac diameters at the sealing zones (respectively D1, D2 and D3), clock position of each target vessel or lengths of interest (RR1, RR2, IRR, L1, L2 and L3). Correlations values are provided Table II.

2) Reproducibility between operators and reference measurements (External assessment)

No statistical difference was depicted between mean values measured by the three operators and data provided by the planning center on the Aquarius workstation (Table III).

3) Comparison between the two workstations (Intra-observer variability between Aquarius and EA-AW)

Interclass correlation between measurements on the two workstations for each operator was respectively 0.918, 0.816, and 0.816 (Table IV).

Inter-observer Variability

Inter-observer agreement was found to be almost identical when comparing mean measures performed by the three operators on both workstations (Table V).

Diameters Analyses

Mean values of the aortic diameter at the proximal sealing zone measured by the three operators on the EA-AW, the Aquarius and provided by the planning center were 29.72 (+/- 3.25) mm, 29.34 (+/- 3.36) and 29.92 (+/- 2.97), respectively. ANOVA did not reveal any statistically significant difference between the three groups ($F = 0.25$; $p = 0.78$). An independent-samples *t*-test was conducted to compare aortic diameters between measurements performed on the EA-AW and the Aquarius by the operators. There was no significant difference in scores ($p = .66$). Similarly, there was no significant difference in scores for right ($p = .64$) and left ($p = .65$) iliac diameters.

Lengths Analyses

No difference was depicted between operators on the two workstations regarding the mean values of the infrarenal aorta (L1) ($p = 0.80$) or the right common iliac artery (L2, L3) ($p = 0.75$) and the left common iliac artery lengths ($p = 0.98$).

Clock Position of Target Vessels

There was no significant variation in clock-position measurements between operators on the

Evaluation of a new imaging software for aortic endograft planning

Table III. Correlation between the operators (mean value for the 3 operators) and data provided by the planning center. (* $p < .00005$ for all comparisons). ICC, interclass correlation coefficients. CT: Celiac Trunk, SMA: Superior Mesenteric Artery, RR: Right Renal, LR: Left Renal.

Measures		ICC (CI 95%)*
Clock Positions (Absolute rate)	CT	.87 (.71-.94)
	SMA	.91 (.80-.96)
	RR	.83 (.64-.92)
	LR	.89 (.75-.95)
Clock positions (SMA °0)	cp-CT	.86 (.69-.93)
	cp-RR	.79 (.55-.90)
	cp-LR	.88 (.74-.94)
Distance between SMA renal arteries	R1	.94 (.87-.97)
	R2	.97 (.93-.98)
	iRR	.85 (.67-.93)
Aortic diameter (proximal sealing zone)	D1	.88 (.78-.94)

Table IV. Comparison of mean values per operator between the two workstations (intra-observer variability between Aquarius and AW) (* $p < .00005$ in all comparisons). ICC, interclass correlation coefficients. CT: Celiac Trunk, SMA: Superior Mesenteric Artery, RR: Right Renal, LR: Left Renal.

Measure		ICC (CI 95%)*		
		1	Observers 2	3
Clock positions (SMA at 0°)	cp-CT	.99 (.99-1.0)	.99 (.99-1.0)	.88 (.76-.94)
	cp-RR	.82 (.60-.91)	.98 (.96-.99)	.90 (.79-.95)
	cp-LR	.86 (.70-.93)	.99 (.99-1.0)	.91 (.81-.96)
Distance between SMA renal arteries	R1	.95 (.90-.98)	.95 (.89-.98)	.93 (.85-.97)
	R2	.92 (.82-.96)	.91 (.80-.96)	.92 (.83-.96)
	iRR	.90 (.79-.96)	.89 (.75-.95)	.90 (.79-.95)
Aortic and iliac diameters (sealing zones)	D1	.89 (.73-.95)	.88 (.65-.95)	.92 (.82-.96)
	D2	.96 (.92-.98)	.94 (.88-.97)	.98 (.96-.99)
	D3	.92 (.84-.96)	.90 (.79-.95)	.89 (.66-.92)
Distance from the lowest renal to the aortoiliac bifurcation Common iliac lengths	L1	.83 (.63-.92)	.75 (.46-.88)	.99 (.98-1.0)
	L2	.99 (.98-1.0)	.99 (.97-.99)	.96 (.92-.98)
	L3	.99 (.97-.99)	.97 (.93-.98)	.99 (.99-1.0)

Table V. Correlation between mean values of the three operators on both workstations (* $p < .00005$ for all comparisons). CT: Celiac Trunk, SMA: Superior Mesenteric Artery, RR: Right Renal, LR: Left Renal.

Measure		Correlation (IC95%)
Clock Positions (Absolute rate)	CT	.91 (.81-.96)
	SMA	.88 (.76-.95)
	RR	.91 (.81-.96)
	LR	.82 (.62-.92)
Clock positions (SMA at 0°)	cp-CT	.95 (.88-.97)
	cp-RR	.81 (.60-.91)
	cp-LR	.77 (.51-.89)
Distance between SMA renal arteries	R1	.97 (.95-.99)
	R2	.99 (.97-.99)
	iRR	.97 (.94-.99)
Aortic and iliac diameters (sealing zones)	D1	.95 (.90-.98)
	D2	.98 (.96-.99)
	D3	.95 (.88-.97)

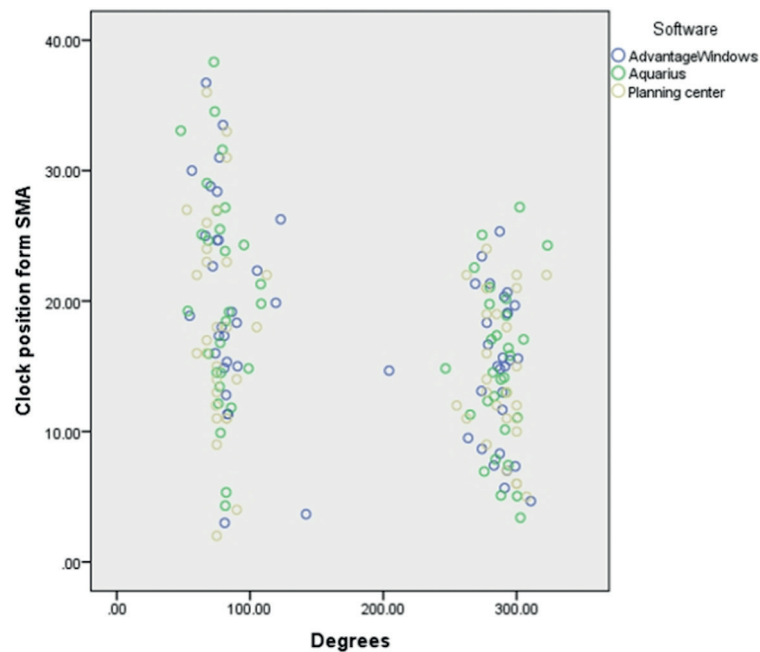


Figure 2. Schematic overview of renal artery positions (with the SMA at 0°, i.e. 12 o'clock position) measured by the three operators on the EA-AW, the Aquarius and provided by the planning center. SMA: Superior Mesenteric Artery, AW: Advantage Windows.

two workstations, with ICC at 0.88 (0.76-0.95) for the SMA, 0.91 (0.81- 0.96) for the RRA and 0.82 (0.62-0.92) for the LRA, respectively. The median and interquartile range was 77.3 (72.2-82.5) degrees for the left RA and 289.3 (277.5-295.0) degrees for the right RA. ANOVA did not reveal any statistically significant differences between two software and the planning center data ($F = 0.95$; $p = 0.45$). Mean length (and SD) for right renal to SMA measured with the EA-AW, the Aquarius or by the PC, were 15.11 (± 5.40), 15.11 (± 5.94) and 14.41 (± 5.50) mm, respectively. The ANOVA test did not reveal any statistically significant differences between groups ($F = 0.03$; $p = 0.97$). Likewise, no differences were found for left renal to SMA length: 20.01 (± 8.74), 20.18 (± 9.48) and 17.41 (± 9.36) mm, respectively ($F = 0.81$; $p = 0.45$). A schematic overview of renal arteries positions assuming the SMA is at 0° (12 o'clock position) is presented in Figure 2.

Discussion

Planning of complex endografts for the treatment of aortic aneurysms is a challenging process that requires high quality pre-operative imaging, access to a dedicated 3D workstation and experience. Each

step requires human interaction, and is therefore associated with a risk of error. Therefore, standardization and computer-assisted semi-automation of this process is useful to ensure reproducibility and reduction of error margins. To perform an accurate sizing, good quality preoperative CT-scan is mandatory (1 mm slice- thickness with an arterial phase). Analysis of consecutive axial slices on a standard computer can be used to confirm the diagnostic of aortic aneurysm. A quick analysis of the aortic anatomy is possible, but fine analyses of the anatomy to check the feasibility of an endovascular repair require post-treatment of the axial raw images. The use of 3DWS to analyze preoperative images and to perform a reliable planning is now considered a standard of care^{1,2,10}. The first step is usually based on a multiplanar and 3D reconstructions analysis. Multiplanar reconstructions provide a rapid overview of the aneurysm anatomy in axial, sagittal and coronal views. 3D reconstructions are useful to evaluate tortuosity and calcifications. It provides physicians with a first opinion regarding treatment options and endovascular accesses. Planning of an endograft is usually performed with manual or semi-automated generation of centerlines of flow (CLF) to avoid parallax error^{6,11,12}. CLFs will be used to check lengths and diameters of the landing zones, and of the endograft, with reproducible measurements between

en operators. Preoperative computed tomography angiography (CTA) image fusion with live fluoroscopy provides a “3D roadmap” that facilitates endovascular navigation and endograft implantation^{13,14}. Fusion has shown to reduce dose and contrast loads during standard and complex EVAR^{7,8}. Endograft planning and fusion mask preparation share a common basis of preoperative images analysis work. During endograft planning, experienced physicians can anticipate many difficulties that could occur during the procedure, such as a tough access to a target vessel due to the presence of calcifications at its origin. However, most of that information is usually lost between the endograft planning and the day of the procedure because they are performed at two different times. This results in additional work and loss of time and information. A new software tool package was recently introduced on the EA-AW workstation. Unlike traditional radiology software tools for vessels measurements, this one was designed in collaboration with our group to fit well with endovascular surgery daily practice. This integrated solution includes both the sizing process and the preparation of the fusion masks and of “best working positions” of the gantry to facilitate regular and complex EVAR procedures (Flight plan for EVAR, GE Healthcare). It was mandatory to check that the sizing tool was “as accurate” as our gold standard Aquarius software. In this study, intra and inter observer variability were

really low, confirming the reliability of the different operators. The ICC comparisons between EA-AW and Aquarius were excellent (> 0.8 for both), thus confirming the reproducibility and reliability of the new EA-AW application. Indeed, aortic and iliac necks diameters and lengths were similarly reported with both workstations, and variations in target vessel measurements for fenestrated stent-graft planning were even less than previously reported in the literature¹⁵. One of the major advantages associated with this new workflow is the integration of planning steps for the procedure, in addition to the endograft planning tool. After conception of the endograft, the operator is invited to design the fusion masks of the bone and vascular structures that will be superimposed to the fluoroscopic images during the procedure. Moreover, all information collected during the endograft planning, such as the best working positions to get access to a target vessel, for example, or the location of a reentry tear in a chronic dissection case (Figure 3), can be implemented onto the fusion mask and stored until the day of the procedure.

Conclusions

Direct comparison of this new software to a dedicated and trusted workstation showed good intra and inter-operators correlations, suggesting

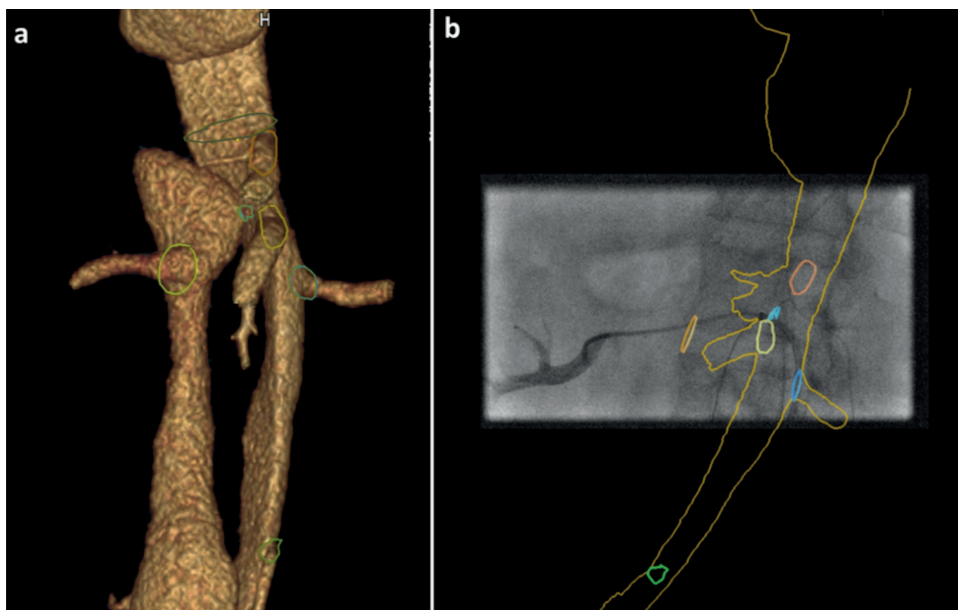


Figure 3. Fusion masks are automatically generated at the end of the endograft planning (EVAR Assist). All information collected during the previous phases, such as the best working angulations or planning lines for the origin of target vessels or reentry tears (in dissection cases) are implemented onto the 3D vascular model *(a)* and stored until the day of the procedure *(b)*.

that it is applicable in clinical practice for designing complex aortic endografts. Moreover, the major input of this new software is represented by the integrated workflow from endograft sizing to procedure planning that should avoid loss of time and information between phases.

Conflict of interest

AH and SH are consultants for GE Healthcare. Lille Aortic Centre received research grants from Terarecon.

References

- 1) SOBOCINSKI J, CHENORHOKIAN H, MAUREL B, MIDULLA M, HERTAULT A, LE ROUX M, AZZAOU R, HAULON S. The benefits of EVAR planning using a 3D workstation. *Eur J Vasc Endovasc Surg* 2013; 46: 418-423.
- 2) PARKER MV, O'DONNELL SD, CHANG AS, JOHNSON CA, GILLESPIE DL, GOFF JM, RASMUSSEN TE, RICH NM. What imaging studies are necessary for abdominal aortic endograft sizing? A prospective blinded study using conventional computed tomography, aortography, and three-dimensional computed tomography. *J Vasc Surg* 2005; 41: 199-205.
- 3) AZZAOU R, SOBOCINSKI J, MAUREL B, D'ELIA P, PERROT C, BIANCHINI A, GUILLOU M, HAULON S. Anatomic study of juxta renal aneurysms: impact on fenestrated stent-grafts. *Ann Vasc Surg* 2011; 25: 315-321.
- 4) LEE WA. Endovascular abdominal aortic aneurysm sizing and case planning using the TeraRecon Aquarius workstation. *Vasc Endovascular Surg* 2007; 41: 61-67.
- 5) GOEL VR, GREENBERG RK, GREENBERG DP. Mathematical analysis of DICOM CT datasets: can endograft sizing be automated for complex anatomy? *J Vasc Surg* 2008; 47: 1306-1312.
- 6) MÜLLER-ESCHNER M, RENGIER F, PARTOVI S, WEBER TF, KOPP-SCHNEIDER A, GEISBÜSCH P, KAUCZOR HU, VON TENGG-KOBLIGK H. Accuracy and variability of semi-automatic centerline analysis versus manual aortic measurement techniques for TEVAR. *Eur J Vasc Endovasc Surg* 2013; 45: 241-247.
- 7) HERTAULT A, MAUREL B, SOBOCINSKI J, MARTIN GONZALEZ T, LE ROUX M, AZZAOU R, MIDULLA M, HAULON S. Impact of hybrid rooms with image fusion on radiation exposure during endovascular aortic repair. *Eur J Vasc Endovasc Surg* 2014; 48: 382-390.
- 8) TACHER V, LIN M, DESGRANGES P, DEUX J-F, GRÜNHAGEN T, BECOUEMIN J-P, LUCIANI A, RAHMOUNI A, KOBEITER H. Image guidance for endovascular repair of complex aortic aneurysms: comparison of two-dimensional and three-dimensional angiography and image fusion. *J Vasc Interv Radiol* 2013; 24: 1698-1706.
- 9) BOSSUYT PM, REITSMA JB, BRUNS DE, GATSONIS CA, GLAZIOU PP, IRWIG LM, LIJMER JG, MOHER D, RENNIE D, DE VET HC, STARD GROUP. Toward complete and accurate reporting of studies of diagnostic accuracy: the STARD initiative. *Acad Radiol* 2003; 10: 664-669.
- 10) SPROUSE LR, MEIER GH, PARENT FN, DEMASI RJ, STOKES GK, LESAR CJ, MARCINCZYK MJ, MENDOZA B. Is three-dimensional computed tomography reconstruction justified before endovascular aortic aneurysm repair? *J Vasc Surg* 2004; 40: 443-447.
- 11) VELAZQUEZ OC, WOO EY, CARPENTER JP, GOLDEN MA, BARKER CF, FAIRMAN RM. Decreased use of iliac extensions and reduced graft junctions with software-assisted centerline measurements in selection of endograft components for endovascular aneurysm repair. *J Vasc Surg* 2004; 40: 222-227.
- 12) AZIZ I, LEE J, LEE JT, DONAYRE CE, WALOT I, KOPCHOK G, MIRAHASHEMI S, ESMALZADEH H, WHITE RA. Accuracy of three-dimensional simulation in the sizing of aortic endoluminal devices. *Ann Vasc Surg* 2003; 17: 129-136.
- 13) ABI-JAOUDEH N, KRUECKER J, KADOURY S, KOBEITER H, VENKATESAN AM, LEVY E, WOOD BJ. Multimodality image fusion-guided procedures: technique, accuracy, and applications. *Cardiovasc Intervent Radiol* 2012; 35: 986-998.
- 14) MARKELJ P, TOMAŽEVIČ D, LIKAR B, PERNUŠ F. A review of 3D/2D registration methods for image-guided interventions. *Med Image Anal* 2012; 16: 642-661.
- 15) OSHIN OA, ENGLAND A, McWILLIAMS RG, BRENNAN JA, FISHER RK, VALLABHANENI SR. Intra- and interobserver variability of target vessel measurement for fenestrated endovascular aneurysm repair. *J Endovasc Ther* 2010; 17: 402-417.